IEEE Access
Multidisciplinary | Rapid Review | Open Access Journal

Received July 15, 2019, accepted August 5, 2019, date of publication August 15, 2019, date of current version September 11, 2019.

Digital Object Identifier 10.1109/ACCESS.2019.2935474

Metal-Frame Antenna for Big-Screen Smartphones Using Characteristic Mode Analysis

BING XIAO[1], (Student Member, IEEE), HANG WONG[2], (Senior Member, IEEE), DI WU[3], (Member, IEEE), AND KWAN L. YEUNG[1], (Senior Member, IEEE)

[1]Department of Electrical and Electronic Engineering, The University of Hong Kong, Hong Kong, China
[2]State Key Laboratory of Terahertz and Millimeter Waves, Department of Electronic Engineering, Shenzhen Research Institute, City University of Hong Kong, Hong Kong, China
[3]College of Electronic Science and Technology, Shenzhen University, Shenzhen 518060, China

Corresponding author: Hang Wong (hang.wong@cityu.edu.hk)

This work was supported in part by International Cooperative Research Program of Guangzhou City GDD district under Grant 2017GH21, the Research Grants Council of the Hong Kong SAR, China (Project No. CityU 11266416), and the Fundamental Research Program of Shenzhen City under Grant JCYJ20170818101409914.

ABSTRACT In previously published papers about the metal-frame smartphone antennas, the screen is usually not included in the antenna model. As the big-screen, or even full-screen (also called all-screen or bezel-less) smartphones become the trend in recent and foreseeable future years, the effect of the very close screen to metal-frame antennas becomes prominent, e.g., the antenna's bandwidth is significantly narrowed. In this paper, a metal-frame antenna for the big-screen smartphone covering 824-960 MHz (GSM850/900), 1452-1496 MHz (LTE1500), 1710–2690 MHz (DCS, PCS, UMTS2100, LTE2300/2500), and 3400-3600 MHz (3.5 GHz 5G) is introduced. For the first time, the screen is fully considered, even designed as part of the antenna. The theory of characteristic modes (TCM) is applied in the design method. A prototype is made and measured for verifying the proposed methodology. Some key parameters of this antenna design are also discussed. This methodology helps to improve the degraded performance of smartphone antennas due to the big-screen industrial design.

INDEX TERMS Bezel-less, characteristic modes, full-screen, metal-frame antenna, mobile phone antenna.

I. INTRODUCTION

Smartphones are prevalent nowadays. They are increasingly intelligent and becoming convenient digital assistants in daily life. Ever since the *iPhone 4* in 2010, the metal-frame antennas have been widely used in the smartphone design. This technique effectively expands the size of the antenna, making it no more confined to a small space inside the smartphone body [1].

However, in a recent couple of years, one clear trend for smartphones is the increasing of their screen-to-body ratios. Smartphones with big-screen or even full-screen (also called all-screen or bezel-less) become popular [2]. In these smartphones, the screen's border width is shortened to only a couple of millimeters [3], [4]. Due to the small spacing between the screen and the metal-frame antenna, they are strongly coupled. The antenna's performance is significantly degraded, especially the significantly narrowed bandwidth, as analyzed in [5]. In Section III of this paper, this conclusion is also validated by the characteristic mode analysis. This result theoretically proves the common experience of antenna designers that the narrower the screen's spacing, the more difficult to achieve wide bandwidth of the metal-frame antennas in big-screen smartphones [6]. Thus, this problem needs to be addressed urgently.

Numerous researches have been conducted on metal-frame smartphone antennas [7]–[14]. To the authors' best knowledge, the screen panel has not been considered independently in these designs. One possible reason is that previously the screen is far from the metal-frame, e.g. 10 mm. The effect of the screen could, to some extent, be neglected. In this condition, the classical PIFA, monopole, or loop antenna theory [15] could be directly applied in analyzing these antennas. However, for antennas in big-screen smartphones, due to the non-negligible electromagnetic effect of the screen panel, the antenna's ''ground'' of single-layer printed circuit board (PCB) turns to the ''ground'' of the connected parallel screen and PCB. In this situation, it is not suitable to apply the

The associate editor coordinating the review of this article and approving it for publication was Hassan Tariq Chattha.

classical analysis methods directly. Based on the above reason, we resort to the theory of characteristic modes (TCM).

In this paper, we proposed the methodology of antenna design for big-screen smartphones by TCM. The antenna has the chassis modes (CMs) and the frame modes (FMs). All the modes of these two kinds are analyzed. Then, we selectively excited the above-mentioned CMs and FMs. By merging the characteristic modes [16], [17], the narrowed bandwidth affected by the screen panel could be expanded again. The simulated and measured results show this antenna can cover the frequency bands of 824-960 MHz (GSM850/900), 1452-1496 MHz (LTE1500), 1710–2690 MHz (DCS, PCS, UMTS2100, LTE2300/2500), and 3400-3600 MHz (3.5 GHz 5G). The gap widths of the screen and the copper clad PCB to the metal frame are compared in Table 1 between the existing literature and the proposed one. The antenna efficiencies are also compared.

TABLE 1. Summary of gap width of metal-frame and efficiency of some smartphone antennas.

	Gap width of Screen (Unit: mm)	Gap width of copper clad PCB (Unit: mm)	Antenna efficiency in Free space
[7]	N/A	10, and 2	>42% >51%
[10]	N/A	7, and 2	>54%
[13]	N/A	12, 7, and 2	62–79% >60%
[14]	N/A	7, and 2	>42% 50–72%
Proposed	**6, and 1**	**5, and 4**	>48%

This method devotes a simple structure to the final deliverable of the multiple-band antenna. It gives the advantage for expanding the narrowed operating bandwidth due to the very close screen for present big-screen smartphone antennas.

II. CHARACTERISTIC MODE ANALYSIS

TCM is firstly developed by Garbacz and then refined by Harrington and Mautz [18], [19]. It could provide the radiating modes of an arbitrarily-shaped metallic structure, without considering the feeding arrangement. These radiating modes, known as characteristic modes, bring physical insight into the radiating phenomena of the antenna [16], [20], [21]. Characteristic modes are obtained by solving an eigenvalue equation that is derived from the method of moments.

$$\mathrm{X}(\mathbf{J}_n) = \lambda_n \mathrm{R}(\mathbf{J}_n) \tag{1}$$

where X and R are the imaginary and real parts of an impedance matrix Z. $\boldsymbol{J}_\mathrm{n}$ denotes the eigencurrent of n-th mode on the structure, and λ_n is the corresponding eigenvalue. The current on a conductive surface can be expressed as a linear superposition of the normalized eigencurrents. The corresponding characteristic angle can be computed from

$$\alpha_n = 180^\circ - \arctan \lambda_n \tag{2}$$

At a given frequency, we can determine whether or not characteristic modes are good radiators by looking at their characteristic angles. When the eigenvalue λ_n approaches zero, or the characteristic angle approaches 180°, the mode is at resonance.

Present smartphones have different sizes and inner structures. In this paper, we generally make *iPhone 8*, which is released in 2017 [22], as a reference for the basic structures. In this smartphone, the screen assembly and the system PCB are separated with a certain distance. The screen almost takes the whole front side of the smartphone. The system PCB is fixed by metallic screws to the rectangular metallic middle frame for good grounding. The size of the middle frame is almost the same as the smartphone's external length and width. From this structure, we can see that for many smartphones, even though the size of the system PCB is getting smaller and smaller, the ground of the antenna model could still be analyzed as full size. The definition of the antenna's ground has expanded from the system PCB to the smartphone's metallic middle frame. However, in this paper, we still use the name of PCB for the continuity of terminologies in academic studies.

For this structure, the antenna will have both chassis modes and frame modes:

A. THE CHASSIS MODES

The screen of smartphones is usually a rectangularly shaped structure with only two or three millimeters thick, but assembled by multiple layers, including the glass cover, touch panel, liquid crystal display (LCD), backlight, and metal cover plate (from outside to inside), which make the screen a sandwich structure. As analyzed in [5], this multi-layer screen assembly is simplified and modeled as a single layer PCB.

The screen panel is parallel and above to the system PCB and electrically connects the PCB by the flexible printed circuit (FPC). FPCs are widely used for interconnecting components to transmit and receive signals in consumer electronic products. In this paper, the FPC is simplified and modeled as a conductive narrow strip connecting the screen and the PCB [5]. The external height and width of this smartphone model are 129 mm by 67 mm. For the initial characteristic mode analysis, the size of the screen is set as 127 mm by 55 mm. The size of the PCB is 124 mm by 57 mm.

1) THE ANTENNA'S GROUND: FROM SINGLE LAYER TO CONNECTED PARALLEL TWO LAYERS

Previously, the researches on smartphone antennas are all based on a single-layer PCB. It serves as the antenna's ground [15]. This chassis plays an important role in the smartphone antenna design [23]. However, for big-screen smartphones, due to the screen's large size, the single-layer "ground" turns to the "ground" of two connected parallel plates. This change to the shape of the smartphone chassis will bring different and new resonating characteristic modes.

For general smartphones, the normalized eigencurrent distributions of the lowest three single PCB modes (PMs) are numerically calculated using the CM-solver of CST Microwave Studio [24] and shown in Fig. 1(a). The size of

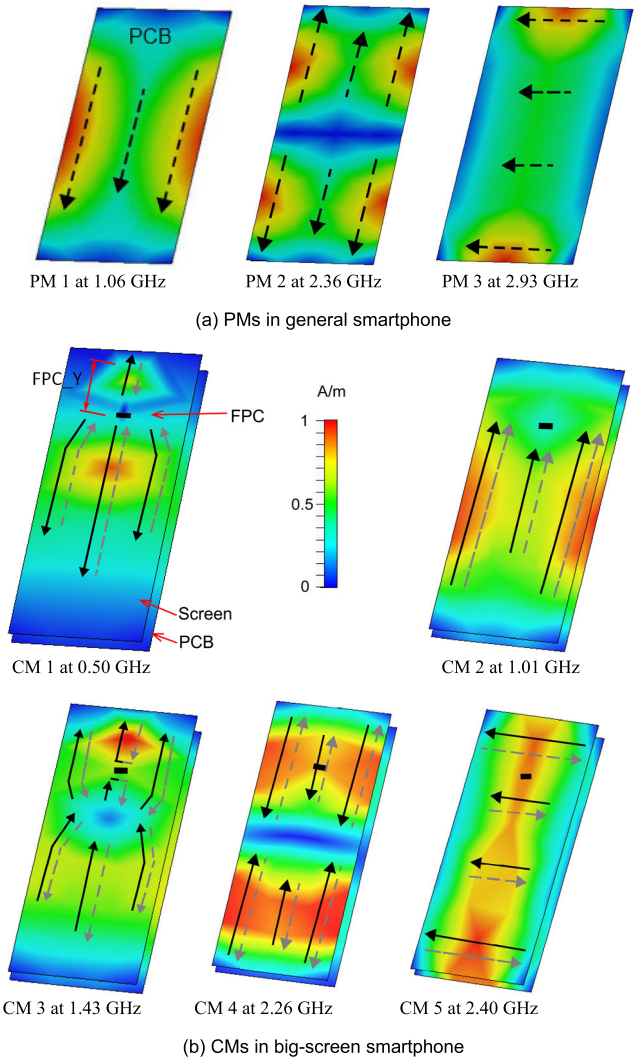

FIGURE 1. **Characteristic currents and corresponding resonating frequencies of (a) single-PCB modes in general smartphone and (b) chassis modes in big-screen smartphone. (In (b), solid arrows are the eigencurrents on the surface of the screen, while the dashed arrows are the eigencurrents on the surface of the PCB.)**

the PCB is 124 mm by 57 mm. The lowest-order mode is a longitudinal 0.5λ-dipole mode. The second mode is a longitudinal 1λ-dipole mode. The third one is a transverse 0.5λ-dipole mode. The results are similar to previous researches of single-layer PCB in general smartphones [25], [26].

However, for big-screen smartphones, the chassis modes (CMs) are no longer equivalent to PMs. As shown in Fig. 1(b), The size of the screen is 127 mm by 55 mm. The distance between the FPC and top edge of the PCB is marked as *FPC_Y*. Here*FPC_Y* is 26 mm. The spacing between the screen and the PCB *h* is 8 mm. Then, the lowest-order mode CM 1 resonates at a much lower frequency of 0.5 GHz due to the connecting FPC. The whole chassis produces a 0.5λ mode. The eigencurrents on the PCB go through the FPC and come back on the screen. The second-order mode CM 2 is similar to PM 1. The directions of the eigencurrents of CM 2 are the same on the screen and the PCB. For the third-order mode CM 3, the eigencurrents go through the FPC. The currents on the screen and the PCB are in opposite directions. CM 4 is similar to PM 2, but the currents on the screen and on the PCB are in opposite directions. CM 5 is similar to PM 3, but the currents on the screen and on the PCB are in opposite directions.

2) THE INFLUENCE OF THE LOCATION OF THE FPC

The size of the chassis and the location of the FPC are factors that affect the resonant frequencies of the CMs. Generally, the sizes of the smartphone's screen and PCB are usually predefined in the Research and Development process, and their influence are obvious. However, the location of the FPC could be moved in a certain range, and its impact is unclear until now.

Fig. 2 shows the influence of characteristic angles with varying *FPC_Y*, from 6 mm to 46 mm with an interval of 10 mm. For CMs 2, 4, and 5, the influence is not obvious. But for CM 1 and CM 3, which are two new modes introduced by the FPC, they are significantly affected.

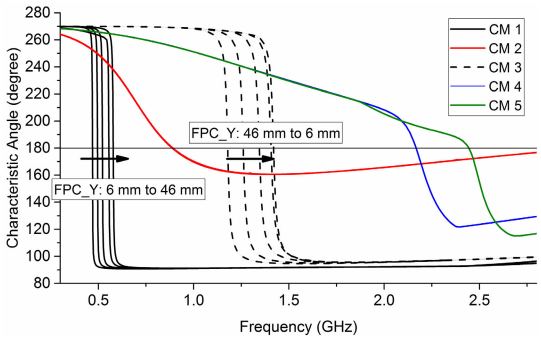

FIGURE 2. **Influence of characteristic angles with varying *FPC_Y*.**

For CM 1, as shown in Fig. 1(b), the eigencurrents go along the PCB, through the FPC, go backward on the screen. The FPC is in the middle of this half-wavelength current path. So, the larger the *FPC_Y*, the lower the FPC's location, the shorter the current paths, the higher the resonant frequency.

For CM 3, also shown in Fig. 1(b), the eigencurrents, on both the screen and the PCB, are distorted by the FPC, and thus the current paths are extended by the FPC. When the *FPC_Y* is smaller, the location of the FPC is higher, this distortion is weaker, the current paths are shorter, so the resonant frequency is higher.

B. CHARACTERISTIC MODES OF THE INTEGRATION OF CHASSIS AND METAL FRAME

Based on the chassis modes analyzed above, we have acquired some resonating frequencies. But they are far from covering all the desired frequency bands. So, the metal frame is then set to surround the upper half of the smartphone for more resonating frequencies to cover the desired several frequency bands. We arrange two grounding points to the metal frame, separating the metal frame into three parts. The middle part is a half loop. Different lengths are extended at

both ends of the half loop in order to produce more resonant modes, as shown in Fig. 4(a). Thus, this configuration makes the metal frame a deformed loop antenna.

Then the characteristic modes of the integration of the chassis and the metal frame are calculated using the CM-solver of CST Microwave Studio [24]. The result of characteristic angles versus frequency is shown in Fig. 3. Only modes resonating below 2.8 GHz are shown. Characteristic eigencurrents of each mode are shown in Fig. 4. It is observed by the eigencurrents that previously analyzed chassis modes still exist in this integration of the metal frame and the chassis. Other newly-produced characteristic modes are frame modes judged by the characteristic eigencurrents. For a better look at the current of the frame modes, the screens are shown in transparent for Fig. 4(c).

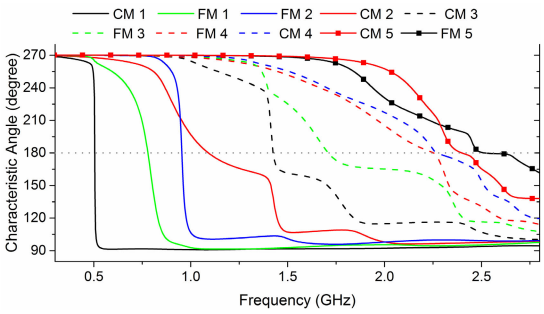

FIGURE 3. Characteristic angles versus frequency for the integration.

The five frame modes resonating below 2.8 GHz are shown in Fig. 5. The resonating frequencies of frame modes can be changed by varying the length of each segment of the frame. FM 1 is a quarter-wavelength monopole mode resonating at 0.86 GHz. FM 2 is a three-quarter-wavelength monopole mode resonating at 1.02 GHz. FM 3 is a one-and-a-quarter-wavelength monopole mode resonating at 1.70 GHz. FM 4 is a one-and-a-half-wavelength mode resonating at 2.03 GHz. FM 5 is a two-wavelength mode resonating at 2.70 GHz.

C. ADDITIONAL MODES

In Fig. 4, we can see for this structure, no characteristic modes are resonating in the frequency band from 1.8 GHz to 2.2 GHz. So, a monopole stub is added on the PCB resonating at around 2 GHz, as shown in Fig. 6(a). Besides, in order to cover 3.4-3.6 GHz frequency band, which is a frequency band for 5G communication under 6 GHz [27], One frame mode of FM 6 is found resonating at 3.5 GHz. It is a three-wavelength mode, as shown in Fig. 7(b).

III. INFLUENCE OF THE SPACING BETWEEN SCREEN AND METAL FRAME

A narrower spacing between the screen and the metal-frame has always been pursued by smartphone manufacturers, because it is necessary for the implementation of a high screen-to-body ratio smartphone. In [5], the influence of the spacing between the metal frame and the screen is given. The bandwidth of the metal-frame antenna will be significantly narrowed as the spacing decreases, from infinity

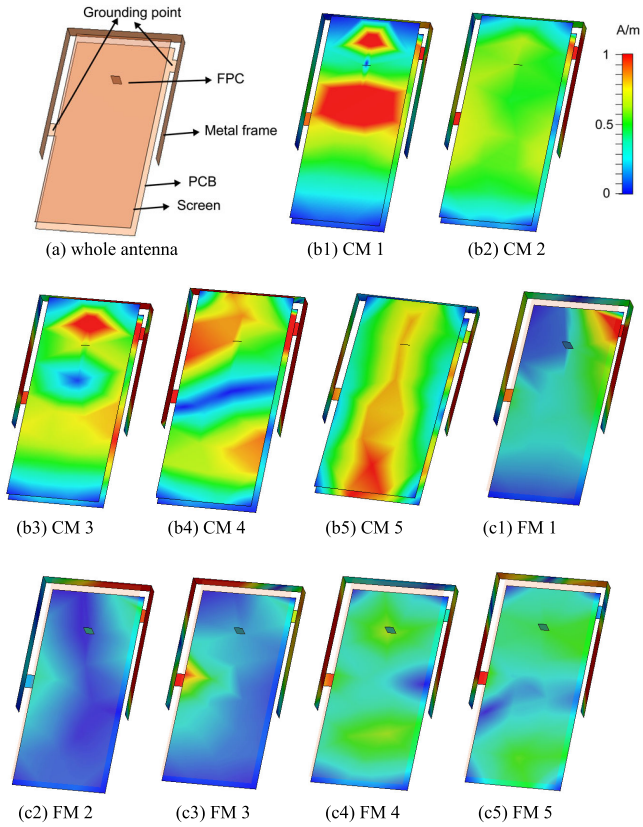

FIGURE 4. Characteristic eigencurrents of (b) CMs and (c) FMs of (a) the whole antenna.

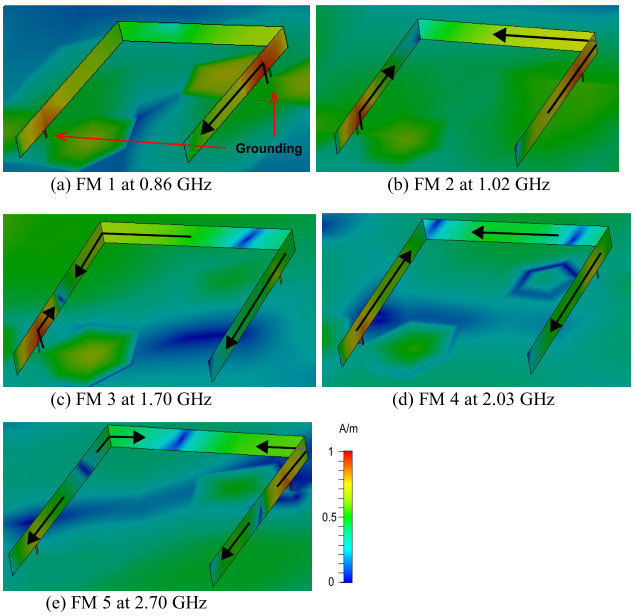

FIGURE 5. Frame modes (FMs).

(the condition of ignoring the screen) to 5 mm to 1 mm. It is because of the large capacitance introduced by the narrow spacing. In industry, when the bandwidth is narrowed by the very close screen, antenna switches [28] or open/closed-loop tuners [29]–[31] are usually used to expand the achievable antenna bandwidth to cover the required frequency bands.

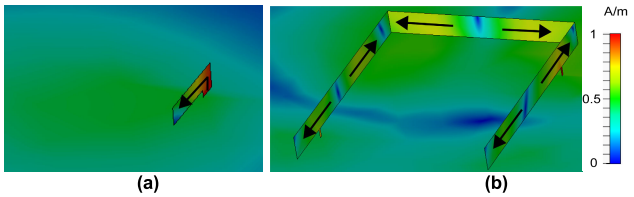

FIGURE 6. Additional Modes of (a) monopole stub resonating at 2 GHz and (b) FM 6 resonating at 3.50 GHz.

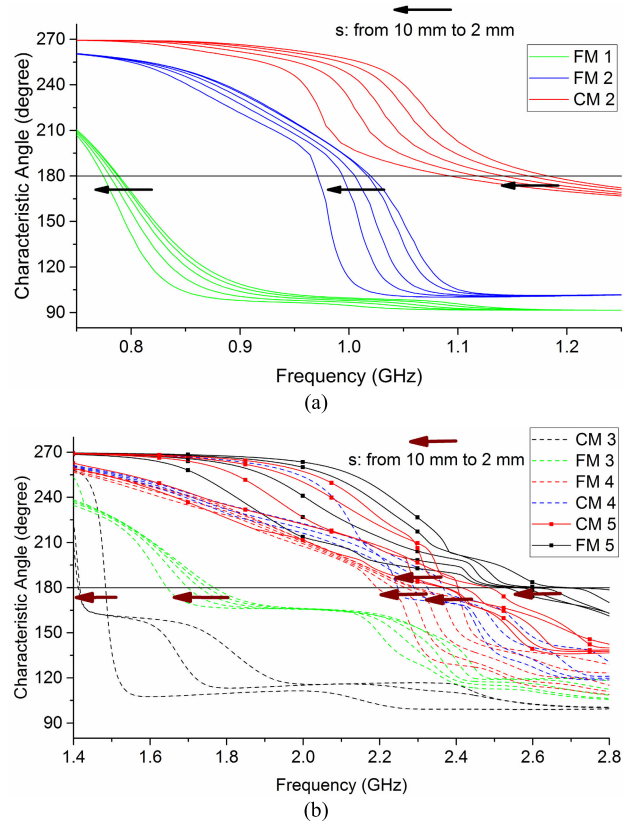

FIGURE 7. Characteristic angles versus the spacing *s* between the screen and the metal frame from 10 mm to 2 mm in (a) 0.85 – 1.25 GHz, (b) 1.4 – 2.8 GHz.

In order to verify this conclusion, we analyzed the influence of *s*, the spacing between the screen and the metal frame, to the radiation bandwidth of the resonant modes in this antenna model. It can be obtained from the slope at 180° of the curve of the characteristic angle. The steeper the slope, the narrower the bandwidth of the corresponding mode [26].

Fig. 7 shows the characteristic angles versus *s*. From 10 mm to 2 mm, the slopes of almost all the modes' characteristic angles, are getting steeper, indicating the bandwidth potential is decreasing. The results theoretically prove the conclusion in [5] that the narrower the spacing, the more difficult to achieve wide bandwidth of the metal-frame antennas in large-screen smartphones.

IV. EXCITATION

In the above model, the metal frame has two grounding points. For this reason, the whole antenna is a deformed loop antenna. So, a current source could be added to replace one of the grounding points to excite the antenna. This configuration could avoid an additional coupler or slot for exciting, simplifying the antenna structure. In this section, we will select which grounding point to be chosen.

CM 1 resonates at 500 MHz, which is much lower than the lower frequency band 824-960 MHz. So, we will not consider it. CMs 2, 3, 4, and 5 could be selected to excite.

Figs. 4(b2) - (b5) show the characteristic eigencurrents of these four chassis modes. Each characteristic mode has its maxima and minima of the current distribution at specific locations. A specific mode can be inductively excited at the maxima of the eigencurrent distribution [32], [33]. If the left grounding point is replaced by the feeding point, all of them could be excited because they have current maxima at the left grounding points. Otherwise, if the top right grounding point is replaced by the feeding point, CMs 2, 3, and 4 could be excited because they have current maxima at the top right grounding points, But CM 5 will not.

Figs. 4(c1) - (c5) show the characteristic eigencurrents of the five frame modes. For a clear observation of the current distribution on the metal frame, the screen is shown in transparent in the figures. If the left grounding point is replaced by the feeding point, FMs 1, 3, 4, and 5 could be excited because they have current maxima at the left grounding points. Instead, if the top right grounding point is replaced by the feeding point, FM 1 and FM 2 could be excited because they have current maxima at the top right grounding points.

Based on the analysis above, in order to excite more modes, the left grounding point will be replaced by the feeding point.

V. PROTOTYPE AND MEASURED RESULTS

After some fine tuning and adjustment of the dimensions, the detailed structure of the proposed antenna is shown in Fig. 8. The metal frame is noted as *ABCDEF*. The feeding point locates at *Point B*. A shorting pin (the grounding point) locates at *Point E*. *AB* is the part at the left side of feeding point. *BCDE* is the part between the feeding point and the grounding point. *EF* is the part at the right of grounding point. For a better look, the screen is shown in semi-transparent.

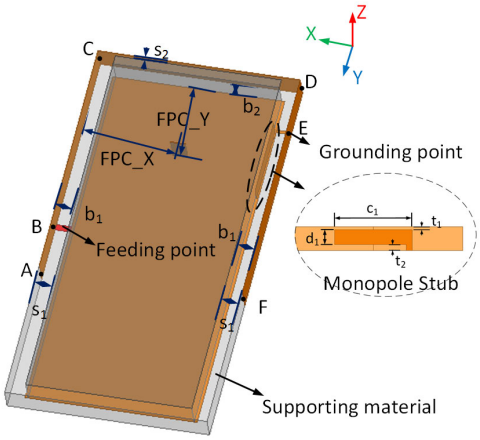

FIGURE 8. The structure and dimensions of the proposed antenna.

In smartphones, sometimes there is also a square loop made of different materials supporting in the inner side of the metal frame. Because the supporting material clings to the metal frame, the material's dielectric constant has an influence on the electrical length, hence the resonant frequencies. Here, for general studies, the supporting material is set as foam, with a dielectric constant of nearly 1.

Two PCBs with single-layer Rogers RT/Duroid 5880 substrate with the thickness of 0.508 mm are used for representing the system PCB and the screen. The size of the system PCB is 124 mm by 57 mm. The size of the screen is 127 mm by 55 mm. The spacing between the screen and the PCB is h. The spacing between the screen and the side edge of the metal frame is s_1. The spacing between the screen and the top edge of the metal frame is s_2. The spacing between the PCB and the side edge of the metal frame is b_1. The spacing between the PCB and the top edge of the metal frame is b_2. The width of the FPC is FPC_w. The detail dimensions are shown in Table 2.

TABLE 2. Dimensions of the proposed antenna.

Dimension	Length (mm)	Dimension	Length (mm)
s_1	6	c_1	26
s_2	1	d_1	5
b_1	5	t_1	1
b_2	4	t_2	2
AB	20	BC	63
CD	67	DE	15.5
EF	66.5	FPC_X	33.5
FPC_Y	26	h	8
FPC_w	5		

A T-shape impedance matching network is designed to tune the antenna. Then a prototype of the proposed antenna was made as shown in Fig. 9. The simulated reflection coefficients of the proposed antenna before and after impedance matching and the measured result are shown in Fig. 10. The corresponding characteristic modes are annotated in the figure. The result exhibits good overall agreement and validates the existence of the modes. The deviations between measured and simulated results may be due to the error of machining accuracy in fabrication.

The radiation performance of the fabricated antenna was measured in SATIMO microwave anechoic chamber. The measured total efficiency and gain are shown in Fig. 11. The measured efficiency is more than 48% in the desired frequency bands. The measured radiation patterns are shown in Fig. 12. In the three mutually orthogonal planes, $\varphi = 0°$, $\varphi = 90°$, and $\theta = 90°$, Co-polarization and Cross-polarization have comparable magnitudes. The obtained result showed that this proposed antenna is applicable to the smartphone design.

It is noteworthy that, the proposed antenna could be further extended to the MIMO dual antenna operation for 4G and 5G communication. In this paper, we used the foam as the supporting material for general studies. If we use supporting materials with higher dielectric constant, such as polycarbonate, which is frequently used in real products, the length

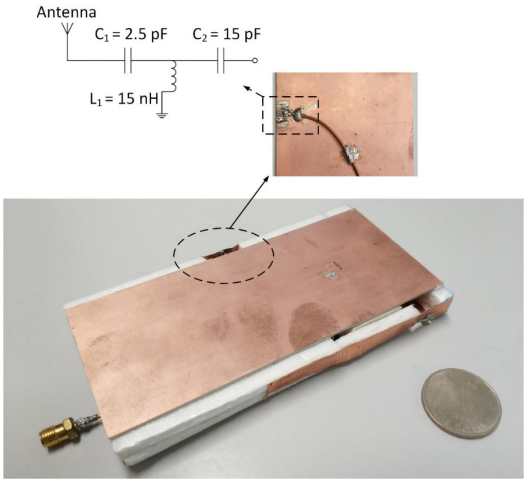

FIGURE 9. The fabricated antenna and the matching network.

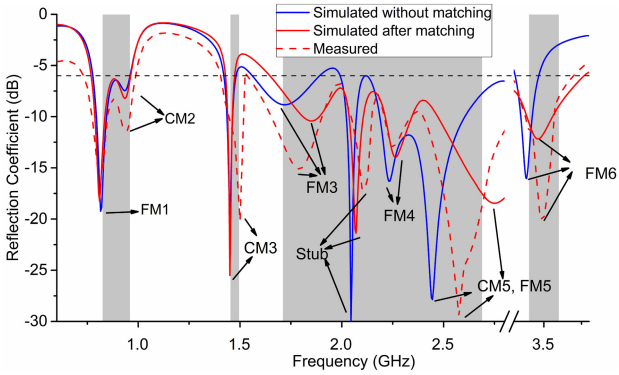

FIGURE 10. Simulated reflection coefficients of the proposed antenna with and without impedance matching and the measured result.

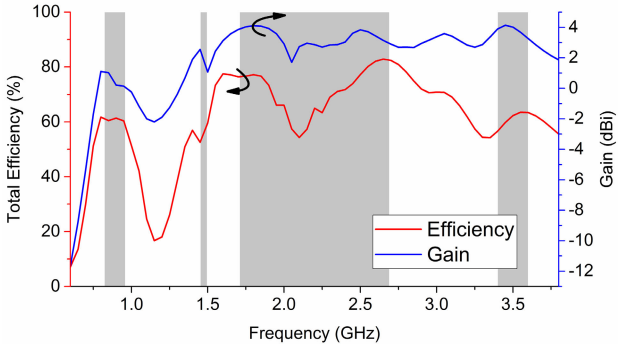

FIGURE 11. Measured total efficiency and gain of the antenna.

of the metal-frame antenna could be shortened. Then the proposed antenna will only take less than half the perimeter of the smartphone body. Thus, the other antenna could be placed in the other half perimeter. Meanwhile, the two MIMO antennas could also be separated at a certain distance which is beneficial for decoupling between them. Furthermore, they could be interposed by grounded metal frame sections to reduce the mutual coupling. Besides, more decoupling methods could be considered to reduce the envelop correlation coefficient (ECC), such as neutralization line [34],

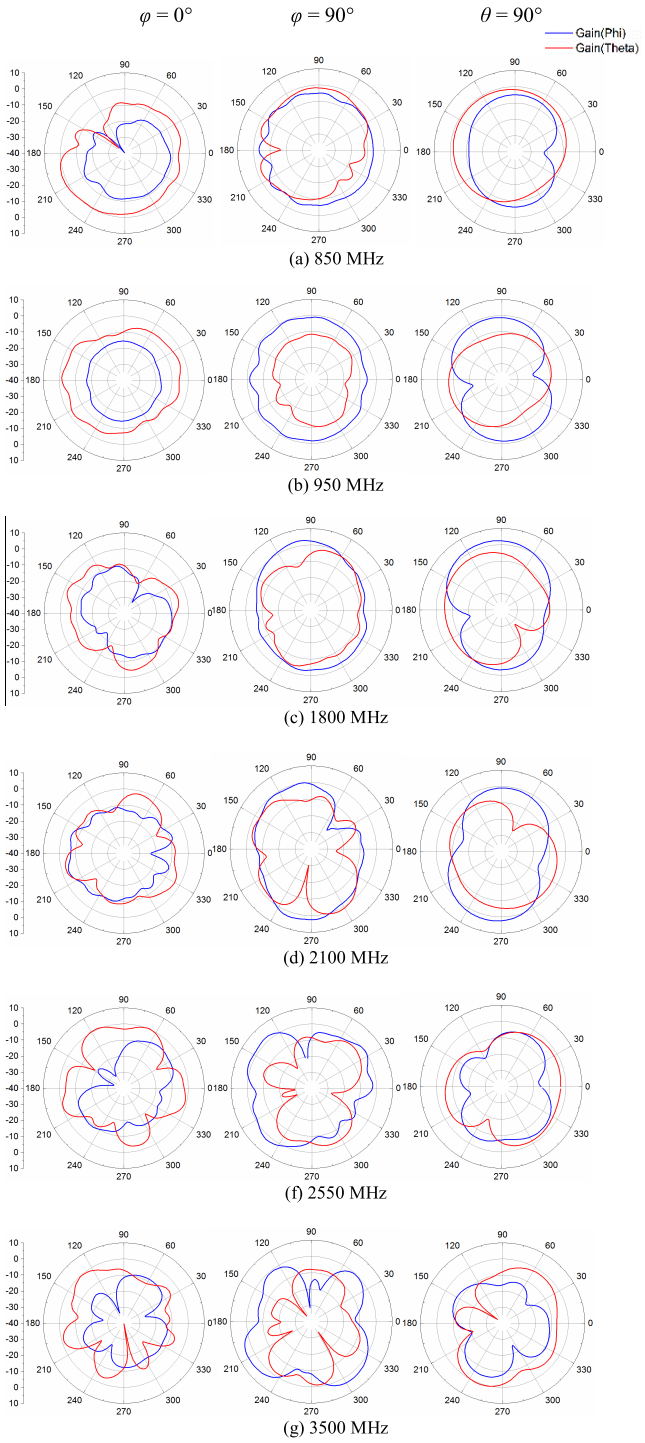

FIGURE 12. Measured radiation patterns.

parasitic decoupling network [35], defected ground structure (DGS) [36], electromagnetic bandgap (EBG) [37], et al.

VI. CONCLUSION

A metal-frame antenna for big-screen smartphones has been proposed by the method of characteristic mode analysis. In big-screen smartphones, the effect of the very close screen significantly narrows the metal-frame antenna's bandwidth. By selectively exciting and merging as many as possible the characteristic modes, the narrowed bandwidth could be expanded to fulfill the GSM/UMTS/LTE/5G requirements. This technique could help to improve the performance of the big-screen smartphone antennas.

REFERENCES

[1] M. Pascolini, R. J. Hill, J. Zavala, N. Jin, Q. Li, R. W. Schlub, and R. Caballero, "Bezel gap antennas," U.S. Patent 8 270 914 B2, Sep. 18, 2012.
[2] J. Callaham. *The Race to 100 Percent: Smartphone Screen-to-Body Ratios Over the Years*. Accessed: Aug. 30, 2019. [Online]. Available: https://www.androidauthority.com/smartphone-screen-to-body-ratio-878835/
[3] Apple (Hong Kong). *iPhone XS—Technical Specifications*. Accessed: Nov. 24, 2018. [Online]. Available: https://www.apple.com/hk/en/iphone-xs/specs/
[4] *Specifications | Samsung Galaxy S9 and S9+, the Official Samsung Galaxy Site*. Accessed: Nov. 24, 2018. [Online]. Available: https://www.samsung.com/global/galaxy/galaxy-s9/specs/
[5] B. Xiao, H. Wong, B. Wang, and K. L. Yeung, "Effect of the screen to metal-frame smartphone antennas," in *Proc. Int. Workshop Antenna Technol. (iWAT)*, 2019, pp. 29–32.
[6] Qorvo Inc. Greensboro, NC, USA. (Feb. 2018). *Overcoming the RF Challenges of Full-Screen Smartphones*. Accessed: Apr. 19, 2019. [Online]. Available: http://www.microwavejournal.com/articles/30336-overcoming-the-rf-challenges-of-full-screen-smartphones
[7] L.-W. Zhang, Y.-L. Ban, C.-Y.-D. Sim, J. Guo, and Z.-F. Yu, "Parallel dual-loop antenna for WWAN/LTE metal-rimmed smartphone," *IEEE Trans. Antennas Propag.*, vol. 66, no. 3, pp. 1217–1226, Mar. 2018.
[8] Y. L. Ban, P.-P. Li, C. Y. D. Sim, and X. Chen, "Dual-feed full-metal-case antenna for WWAN/LTE smartphone applications," *Int. J. RF Microw. Comput.-Aided Eng.*, vol. 26, no. 7, pp. 595–601, 2016.
[9] L.-W. Zhang and Y.-L. Ban, "Novel hepta-band coupled-fed antenna for WWAN/LTE metal-ring-frame smartphone applications," in *Proc. PIERS*, 2014, pp. 2190–2193.
[10] J.-W. Lian, Y.-L. Ban, Y.-L. Yang, L.-W. Zhang, C.-Y.-D. Sim, and K. Kang, "Hybrid multi-mode narrow-frame antenna for WWAN/LTE metal-rimmed smartphone applications," *IEEE Access*, vol. 4, pp. 3991–3998, 2016.
[11] Y. Yan, Y.-L. Ban, G. Wu, and C.-Y.-D. Sim, "Dual-loop antenna with band-stop matching circuit for WWAN/LTE full metal-rimmed smartphone application," *IET Microw., Antennas Propag.*, vol. 10, no. 15, pp. 1715–1720, 2016.
[12] H.-B. Zhang, Y.-L. Ban, Y.-F. Qiang, J. Guo, and Z.-F. Yu, "Reconfigurable loop antenna with two parasitic grounded strips for WWAN/LTE unbroken-metal-rimmed smartphones," *IEEE Access*, vol. 5, pp. 4853–4858, 2017.
[13] Y. L. Ban, Y. F. Qiang, Z. Chen, K. Kang, and J. H. Guo, "A dual-loop antenna design for hepta-band WWAN/LTE metal-rimmed smartphone applications," *IEEE Trans. Antennas Propag.*, vol. 63, no. 1, pp. 48–58, Jan. 2015.
[14] Y.-L. Ban, Y.-F. Qiang, G. Wu, H. Wang, and K.-L. Wong, "Reconfigurable narrow-frame antenna for LTE/WWAN metal-rimmed smartphone applications," *IET Microw. Antennas Propag.*, vol. 10, no. 10, pp. 1092–1100, Apr. 2016.
[15] H. Wong, K.-M. Luk, C. H. Chan, Q. Xue, K. K. So, and H. W. Lai, "Small antennas in wireless communications," *Proc. IEEE*, vol. 100, no. 7, pp. 2109–2121, Jul. 2012.
[16] C. Deng, Z. Feng, and S. V. Hum, "MIMO mobile handset antenna merging characteristic modes for increased bandwidth," *IEEE Trans. Antennas Propag.*, vol. 64, no. 7, pp. 2660–2667, Jul. 2016.
[17] Z. Miers, H. Li, and B. K. Lau, "Design of bandwidth-enhanced and multiband MIMO antennas using characteristic modes," *IEEE Antennas Wireless Propag. Lett.*, vol. 12, pp. 1696–1699, 2013.
[18] R. J. Garbacz and R. Turpin, "A generalized expansion for radiated and scattered fields," *IEEE Trans. Antennas Propag.*, vol. AP-19, no. 3, pp. 348–358, May 1971.
[19] R. F. Harrington and J. R. Mautz, "Theory of characteristic modes for conducting bodies," *IEEE Trans. Antennas Propag.*, vol. 19, no. 5, pp. 622–628, Sep. 1971.
[20] Y. Chen and C.-F. Wang, *Characteristic Modes: Theory and Applications in Antenna Engineering*. Hoboken, NJ, USA: Wiley, 2015.

[21] H. Li, Z. T. Miers, and B. K. Lau, "Design of orthogonal MIMO handset antennas based on characteristic mode manipulation at frequency bands below 1 GHz," *IEEE Trans. Antennas Propag.*, vol. 62, no. 5, pp. 2756–2766, May 2014.
[22] *iPhone 8—Technical Specifications—Apple (HK)*. Accessed: Dec. 19, 2018. [Online]. Available: https://www.apple.com/hk/en/iphone-8/specs/
[23] P. Vainikainen, J. Ollikainen, O. Kivekas, and I. Kelander, "Resonator-based analysis of the combination of mobile handset antenna and chassis," *IEEE Trans. Antennas Propag.*, vol. 50, no. 10, pp. 1433–1444, Oct. 2002.
[24] *CST—Computer Simulation Technology*. Accessed: Dec. 30, 2018. [Online]. Available: https://www.cst.com/
[25] J. Rahola and J. Ollikainen, "Optimal antenna placement for mobile terminals using characteristic mode analysis," in *Proc. 1st Eur. Conf. Antennas Propag.*, Nice, France, 2006, pp. 1–6.
[26] M. Cabedo-Fabres, E. Antonino-Daviu, A. Valero-Nogueira, and M. F. Batalle, "The theory of characteristic modes revisited: A contribution to the design of antennas for modern applications," *IEEE Antennas Propag. Mag.*, vol. 49, no. 5, pp. 52–68, Oct. 2007.
[27] *World Radiocommunication Conference Allocates Spectrum for Future Innovation*. Accessed: Jan. 1, 2019. [Online]. Available: http://www.itu.int/net/pressoffice/press_releases/2015/56.aspx#.XCslz9VLikm
[28] K. R. Boyle and P. G. Steeneken, "A five-band reconfigurable PIFA for mobile phones," *IEEE Trans. Antennas Propag.*, vol. 55, no. 11, pp. 3300–3309, Nov. 2007.
[29] A. S. Morris, Q. Gu, M. Ozkar, and S. P. Natarajan, "High performance tuners for handsets," in *IEEE MTT-S Int. Microw. Symp. Dig.*, Jun. 2011, pp. 1–4.
[30] K. R. Boyle, E. Spits, M. A. de Jongh, S. Sato, T. Bakker, and A. van Bezooijen, "A self-contained adaptive antenna tuner for mobile phones: Featuring a self-learning calibration procedure," in *Proc. 6th Eur. Conf. Antennas Propag. (EUCAP)*, 2012, pp. 1804–1808.
[31] M. A. de Jongh, A. van Bezooijen, T. Bakker, K. R. Boyle, and J. Stulemeijer, "A low-cost closed-loop antenna tuner module for mobile phone single-feed multi-band antennas," in *Proc. Eur. Microw. Conf.*, 2013, pp. 1171–1174.
[32] R. Martens, E. Safin, and D. Manteuffel, "Inductive and capacitive excitation of the characteristic modes of small terminals," in *Proc. Antennas Propag. Conf. (LAPC)*, Loughborough, U.K., 2011, pp. 1–4.
[33] R. Martens, E. Safin, and D. Manteuffel, "Selective excitation of characteristic modes on small terminals," in *Proc. 5th Eur. Conf. Antennas Propag. (EUCAP)*, 2011, pp. 2492–2496.
[34] Y. Wang and Z. Du, "A wideband printed dual-antenna with three neutralization lines for mobile terminals," *IEEE Trans. Antennas Propag.*, vol. 62, no. 3, pp. 1495–1500, Mar. 2014.
[35] M. Li, L. Jiang, and K. L. Yeung, "Novel and efficient parasitic decoupling network for closely coupled antennas," *IEEE Trans. Antennas Propag.*, vol. 67, no. 6, pp. 3574–3585, Jun. 2019.
[36] D. Wu, X. Hua, S. W. Cheung, B. Wang, M. Li, and B. Xiao, "A compact slot MIMO antenna for smartphones with metal housing," *J. Electromagn. Appl.*, vol. 32, no. 2, pp. 204–214, 2018.
[37] S.-H. Kim, J.-Y. Lee, T. T. Nguyen, and J.-H. Jang, "High-performance MIMO antenna with 1-D EBG ground structures for handset application," *IEEE Antennas Wireless Propag. Lett.*, vol. 12, pp. 1468–1471, 2013.

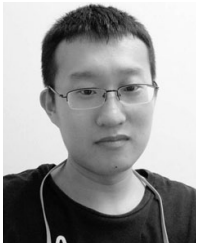

BING XIAO received the B.Sc. degree in applied physics from Anhui University, Hefei, China, in 2009, and the M.Sc. degree in radio physics from the University of Electronic Science and Technology of China (UESTC), Chengdu, China, in 2012. He started his career as an Antenna/RF Engineer with the China Electronics Technology Group Corporation (CETC), in 2012, and then, with Xiaomi Corporation. He is currently pursuing the Ph.D. degree in electronic engineering with The University of Hong Kong, Hong Kong, China. His current research interests include smart devices and the IoT antennas.

HANG WONG (M'06–SM'12) received the B.Eng., M.Phil., and Ph.D. degrees in electronic engineering from the City University of Hong Kong, in 1999, 2002, and 2006, respectively. He was an acting Assistant Professor with the Department of Electrical Engineering, Stanford University, in 2011. He joined the Department of Electronic Engineering, City University of Hong Kong, in 2012, as an Assistant Professor. He had visiting professorships at the University of Waterloo, Canada, University of College London, U.K., and the University of Limoges, France, in 2013, 2014, and 2015, respectively. He has published more than 90 international journals and conference papers. He holds 16 U.S. and Chinese patents. His research interests include design of broadband antennas, small antennas, millimeter-wave antennas, 3D printed antenna, and related applications. He received the 2011 State Technology Invention Award presented by the Ministry of Science and Technology, China, with Professors Kwai-Man Luk, Chi-Hou Chan, and Quan Xue for their contributions of wideband patch antenna developments and applications. He was the Chair of the IEEE Hong Kong Section of the Antennas and Propagation (AP)/Microwave Theory and Techniques (MTT) Chapter, from 2011 to 2014. He is the IEEE APS Region-10 Representative. He has been an Associate Editor of the IEEE Antennas and Wireless Propagation Letters, since 2012.

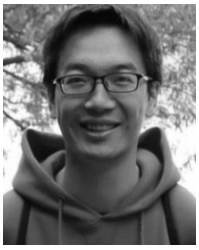

DI WU (M'18) received the B.Eng. degree in electromagnetic field and microwave technology from the University of Electronic Science and Technology of China (UESTC), Chengdu, China, in 2009, the M.S. degree from the City University of Hong Kong, Hong Kong, in 2013, and the Ph.D. degree from The University of Hong Kong, Hong Kong, in 2018.

In 2017, he was a Visiting Ph.D. Student with the University of Wisconsin-Madison, Madison, WI, USA. From 2010 to 2012, he was with MediaTek Inc. (MTK), as a Senior RF Engineer. From 2018 to 2019, he was with the Hong Kong Applied Science and Technology Research Institute (ASTRI), Hong Kong, as a Senior System Design Engineer. Since January 2019, he has been with the College of Electronic Science and Technology, Shenzhen University, Shenzhen, China, as an Assistant Professor. His current research interests include phased array systems, phase shifter, antennas, and RF/microwave circuits.

KWAN L. YEUNG (S'93–M'95–SM'99) was born in 1969. He received the B.Eng. and Ph.D. degrees in information engineering from the Chinese University of Hong Kong, in 1992 and 1995, respectively. He joined the Department of Electrical and Electronic Engineering, The University of Hong Kong, in July 2000, where he is currently a Professor. His research interests include next-generation Internet, packet switch/router design, all-optical networks, and wireless data networks.